https://doi.org/10.32604/zkg.2025.04-05.03

CFD-Based Multiphysics Analysis of Coupled Combustion-Decomposition Interactions and NOx Reduction Mechanisms in an NSF-I Type Precalciner

Prof. Shuxia Mei[1], Zhengwu Wan[1], Prof. Junlin Xie[2], Hu Yang[1], Changjiang Liu[3]
[1]School of Materials Science and Engineering, Wuhan University of Technology, Wuhan 430070, China
[2]School of Materials Science and Engineering, Beijing University of Technology, Beijing 100124, China
[3]Hubei Jingrui Optical Co., Ltd., Wuhan 430070, China
Corresponding Author: Prof. Junlin Xie, xjlclxy@126.com

A numerical simulation was carried out for a 6500T/D NSF-I precalciner in a China Resources Cement Plant. The coupling process between coal powder combustion and calcium carbonate decomposition was analyzed, and the mechanism of nitrogen oxide reduction through coal powder staged combustion was revealed. The simulation results are consistent with the measured data, indicating the reliability of the simulation results. The simulation results show that when the fl ue gas fl owing vertically from the bottom meets the tertiary air entering the precalciner in a tangential direction from the side, the two gas streamlines intertwine well and spiral up, resulting in a longer residence time. The pulverized coal in the precalciner is fully burned, and the burn-out rate of each stream of pulverized coal is more than 97%. The decomposition of calcium carbonate is good, with a decomposition rate of up to 96%. The coal powder used for staged combustion in the cone part undergoes incomplete combustion after entering the precalciner, producing a large amount of carbon monoxide, which rapidly reduces the nitrogen oxides entering from the bottom of the precalciner, indicating that the effect of coal staged combustion on reducing nitrogen oxides is significant.

PROCESS

1 Introduction

With the worsening of the Earth's environment, green manufacturing, energy conservation and emission reduction have become necessary for the sustainable development of the cement industry.

In China, the proposed "Emission Standards for Air Pollutants in the Cement Industry" aims to reduce NOx emissions by approximately 980000 t from the current 1.9 - 2.2 million t, representing a reduction of 44.5% - 51.6%. It is evident that achieving this target will be challenging. Therefore, reducing coal consumption and controlling NOx emissions have become mandatory requirements for the cement industry.

The rotary kiln and the precalciner are crucial equipments in the cement production system, requiring substantial coal consumption and serving as the primary source of NOx emissions in cement plants. The rotary kiln is responsible for clinker sintering, while the precalciner handles the raw meal decomposition [1]. However, the NOx generated in the rotary kiln eventually enters the precalciner and escapes from its outlet. Therefore, it is necessary to employ reasonable and effective control methods in the precalciner to reduce NOx emissions. Staged combustion technology is an important approach for effectively controlling NOx emissions in the precalciner, achieving efficient low-NOx combustion in the cement production [2,3]. It has been a focus of research for scholars both domestically and internationally.

Due to the complex internal flow field of the precalciner, which not only involves the interaction between the tertiary air and flue gas, but also involves the coupling between the combustion of pulverized coal and the decomposition of raw meal, a reasonable analysis of the flow field is an important prerequisite for studying the precalciner.

The flow field in the precalciner is very complex, with not only the interaction between the tertiary air and flue gas, but also the coupling between coal combustion and raw meal decomposition. Numerical simulation methods have been widely adopted in the study of the flow field in precalciners. Kolyfetis [4] analyzed the gas phase flow field in an SLC-type precalciner by numerical simulation. Zhao Weilin [5] studied the flow field of different types of precalciners through numerical simulations. Xian L [6,7] et al. used Fluent to simulate the flow field in a precalciner, providing an effective guide for the subsequent work. Yang Yu [8] established a model for the precalciner of a cement plant, simulating the combustion process of pulverized coal and the decomposition process

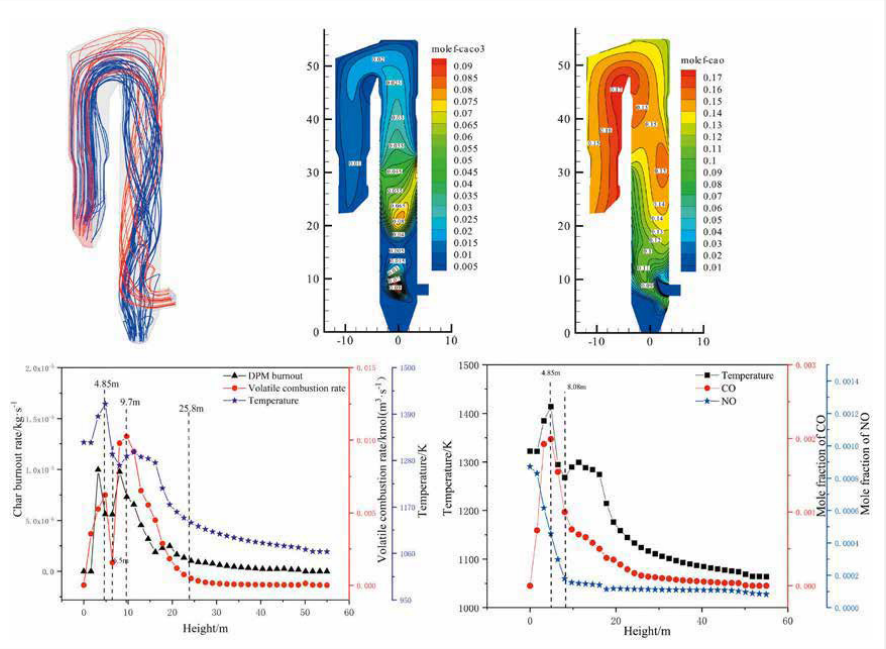

CFD-Based Multiphysics analysis in an NSF-I Type precalciner

of calcium carbonate. Based on the basic flow field in the precalciner, more and more research focus has been shifted to NOx reduction. D Li [9] used a combination of theoretical analysis, simulation experiments and numerical simulations to study the NO generation and reduction pattern, and analysed the distribution characteristics of NOx and reduction products in the precalciner. Bugge [10] et al. systematically investigated the generation of NOx from biomass pellet combustion using numerical simulation and derived the range of air excess coefficients that result in the highest NOx generation. X Zeng [11] investigated the species distributions to elucidate the formation mechanism of self-generated NOx in a precalciner. Yang Y[12,13] et al. optimized the structure and parameters of a precalciner in order to reduce the NOx emission using numerical simulations.

The above mentioned researches indicate that CFD technology is currently the main means of studying the precalciner, but numerical simulation research on the coupling of fuel combustion and raw meal decomposition, as well as the mechanism of nitrogen oxide formation, is still immature, especially for the staged combustion of NSF type precalciner, with relatively little research. In view of this, an NSF-I precalciner of China Resources Cement was numerically simulated. The coupling process of fuel combustion and raw meal decomposition and the mechanism of staged combustion to reduce NOx emission were mainly studied. The research work has an important guiding significance for precalciner to reduce NOx emission by fuel staged combustion.

2 Geometric models and meshes

Figure 1 shows the geometric structure of the precalciner, which is of the NSF-I type and has a production capacity of 6500 t/d. There are three types of inlets, namely gas inlet (flue gas inlet and tertiary air inlet), pulverized coal inlet, and raw meal inlet. The flue gas from the rotary kiln enters the precalciner vertically from the bottom, and the high-temperature tertiary air enters the precalciner in a tangential direction. There are 5 pulverized coal inlets, of which 2 main coal pipes are located near the lower raw meal inlets, and the other 3 coal pipes used for staged combustion are evenly distributed in the lower cone part of the precalciner. There are four inlets of raw meal. The mesh is shown in Figure 2.

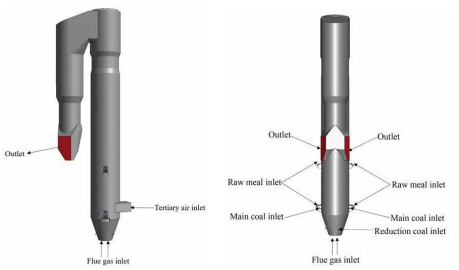

1 Geometric structure

2 Meshes

3 Numerical models

3.1 Gas phase

For the gas-phase model, the Realizable K-ε model is chosen, which has been extensively validated for a wide range of flows and is more realistic in cyclonic calculations.

$$\frac{\partial}{\partial t}(\rho k)+\frac{\partial}{\partial x_j}(\rho k u_j)=\frac{\partial}{\partial x_j}\left[\left(\mu+\frac{\mu_t}{\sigma_k}\right)\frac{\partial k}{\partial x_j}\right] + G_k + G_b - \rho\varepsilon - Y_M + S_k \quad (1)$$

$$\frac{\partial}{\partial t}(\rho k)+\frac{\partial}{\partial x_j}(\rho \varepsilon u_j)=\frac{\partial}{\partial x_j}\left[\left(\mu+\frac{\mu_t}{\sigma_\varepsilon}\right)\frac{\partial \varepsilon}{\partial x_j}\right] + \rho C_2 S\varepsilon - \rho C_2 \frac{\varepsilon^2}{k+\sqrt{v\varepsilon}} + C_{1\varepsilon}\frac{\varepsilon}{k}C_{3\varepsilon}G_b + S_\varepsilon \quad (2)$$

$$C_1 = max[0.43, \frac{\eta}{\eta+5}], \eta = S\frac{k}{\varepsilon}, S=\sqrt{2S_{ij}S_{ij}} \quad (3)$$

In these equations, G_k represents the turbulence kinetic energy generation due to the mean velocity gradients. G_b is the turbulence kinetic energy generation due to the buoyancy. Y_M represents the contribution of the fluctuating dilatation in the compressible turbulence to the overall dissipation rate. C_2 and $C_{1\varepsilon}$ are constants. σ_k and σ_ε are the turbulent Prandtl numbers for k and ε, respectively. S_k and S_ε are user-defined source terms.

3.2 Particle phase

For the particle phase (pulverized coal), the Discrete Phase Model and Discrete Random Walk Model are used to calculate the trajectory of the particle phase. It is assumed that the particles are spherical and the diameter distribution conforms to the Rosin-Rammler distribution, without considering the interaction between pulverized coal particles.

For the pulverized coal combustion process, the Species Transport Model combined with the Finite-Rate/Eddy-Dissipation Model was used. The combustion process of pulverized coal is divided into two parts. Volatiles are first released and burned quickly, during which, the char begins to burn. The single-rate devolatilization model was used for the volatile devolatilization, which assumes that the rate of devolatilization is first-order and depends on the amount of volatiles remaining in the particle.

For char combustion, the kinetic/diffusion surface reaction rate model was used, which assumed that the surface reaction rate was determined either by kinetics or by diffusion rate.

3.3 Raw meal reaction

In addition to $CaCO_3$, the raw meal contains impurities such as clay and sand. Due to the significant proportion of $CaCO_3$ in the raw meal, the research on the decomposition reaction model of the raw meal has predominantly focused on the decomposition of $CaCO_3$ by both domestic and international scholars. The decomposition of $CaCO_3$ involves a series of physical and chemical processes. The physical processes include heat and mass transfer, as well as turbulent diffusion of the decomposition product CO_2, while the chemical processes mainly involve the decomposition reaction where $CaCO_3$ decomposes into CaO and CO_2.

3.4 Methods

The governing equations for the continuous phase are discretized using the finite volume method, and a steady-state pressure-based solver is employed as the solution method. The pressure-velocity coupling algorithm follows the Simple algorithm. The discretization schemes for various parameters are as follows: the pressure is discretized using the PRESTO! scheme, while the remaining parameters utilize second-order upwind schemes. The discretized system of equations is solved using the TDMA method, and each variable is iterated with underrelaxation until convergence is achieved. The relaxation factors for the equations and species are as follows: pressure (0.3), momentum (0.4), density (0.25), body force (0.9), turbulence kinetic energy and dissipation rate (0.75), species (0.75), energy (0.2), and P1 (0.5). The convergence criteria are set as follows: the residual of the energy equation and P1 radiation is less than 10-6, while the residuals of the other equations and species are less than 10^{-3}.

4 Boundary conditions

Real data from the actual operating conditions of the precalciner are used as boundary conditions. The detailed boundary conditions for the velocities of the flue gas and tertiary air, as well as for the amount of raw meal and pulverized coal required are shown in Table 1. The proximate analysis and ultimate analysis of the pulverized coal are shown in Table 2.

Table 1 **Boundary conditions**

Boundary type	Temperature/K	Mass flow rate/kg·s-1	velocity/m·s-1
Flue gas	1368	/	20
Tertiary gas	1198	/	31
raw	1078	96	/
Coal	320	5.6	25

Table 2 **Proximate analysis and ultimate analysis of the coal**

Proximate analysis (ad)/%				Ultimate analysis (ad)/%					Qad/(kJ/kg)
M	A	V	FC	C	H	O	N	S	24189
2	25	30.05	42.95	79.647	4.387	13.563	1.226	1.177	

Table 3 **Comparison between simulated value and measured value**

	Simulated values	Measured values	Relative error
Outlet temperature/K	1050	1140	7.9%
O2/%	3.2	3	6.7%
$CaCO_3$ decomposition rate/%	94	92	0.21%

5 Results and Discussions

5.1 Result Verification

Table 3 presents a comparison between simulated and measured data for the precalciner. The measured data is obtained from the central control room of the cement plant. It can be observed that the error between the simulated values and the actual measured data is extremely small and falls within the allowable range of error for the project. Considering the complexity of clinker calcination, chemical reactions of coal combustion, and the inherent errors in numerical simulation calculations, these results indicate that the simulation results are reasonable.

5.2 Gas flow fields

Figure 3 shows the gas streamlines. Figure 4 displays the velocity vector. From Figure 3 and Figure 4 we can see that, when the vertical upward flue gas meets the tangential tertiary air, they interact with each other and rise spirally through the precalciner. The maximum residence time for the tertiary air and the flue gas is 7.65 s and 13.9 s, respectively.

5.3 Coal combustion

There are five coal pipes in this precalciner, two main coal pipes near the tertiary air inlet and three coal pipes for staged combustion in the cone section at the bottom of the precalciner. When the pulverized coal is sprayed into the high-temperature precalciner, the volatile matter is first released and rapidly burned. During this period, the coke begins to gradually burn.

There are five coal pipes in this precalciner, two main coal pipes near the tertiary air inlet and three coal pipes for staged combustion in the cone section at the bottom of the precalciner. When the pulverized coal is sprayed into the high-temperature precalciner, the volatile matter is first released and rapidly burned. During this period, the coke begins to gradually burn.

Figure 5 shows the trajectories of coal particles colored by static temperature. Figure 6 shows the temperature contours on the central longitudinal sections. As can be seen from Figure 5 and Figure 6, five streams of coal powder are carried by the gas flow and rotate upwards in the precalciner, rapidly burning near the coal pipes to form five local high-temperature zones.

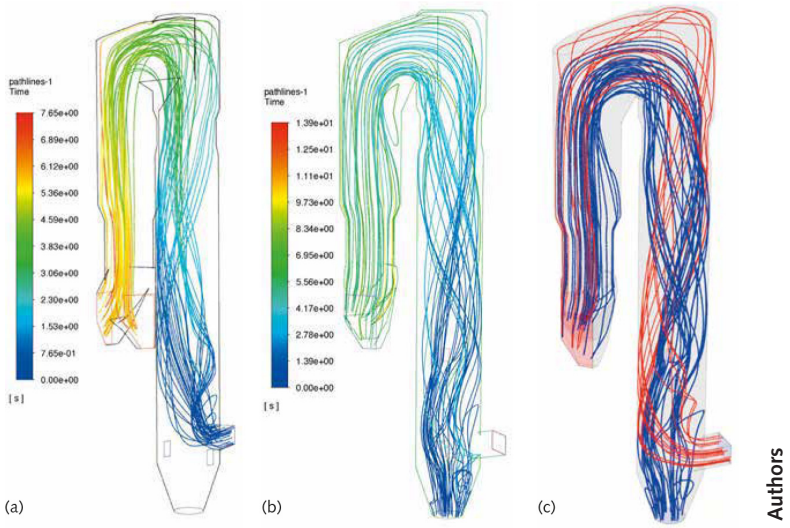

3 **Gas streamlines (a) Tertiary air (b) Flue gas (c) Mixed gas**

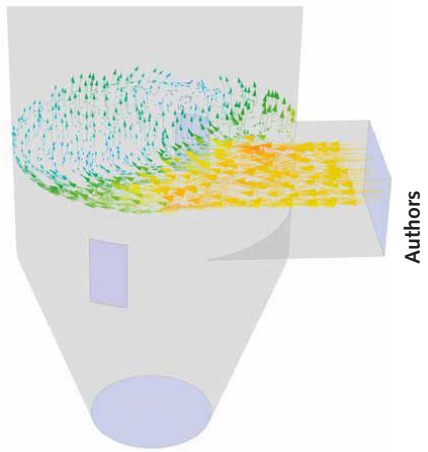

4 **Velocity vector**

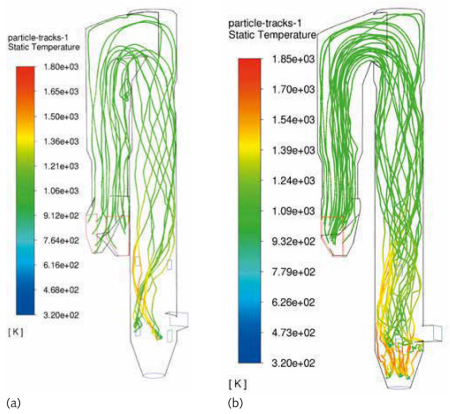

Authors

5 Coal particle trajectories colored by static temperature (a) Two main coal pipes (b) Three coal pipes for grading combustion

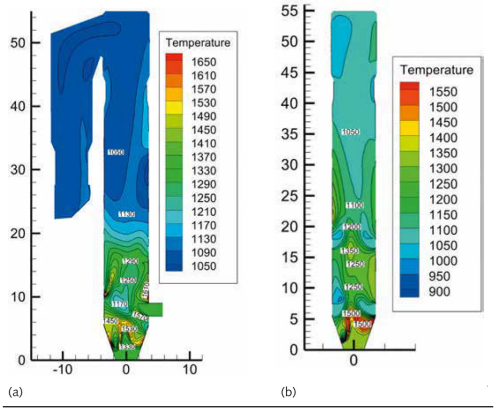

Authors

6 The temperature contours on the central longitudinal sections (a) X=0 (b) Z=0

Figure 7 shows the release rate of volatile matter and Figure 8 displays the average volatile kinetic reaction rate, char burnout rate and temperature along Y direction (the height direction). From Figure 7 and Figure 8 we can see that compared with the two coal powder streams sprayed by two main coal pipes located in the cylinder section, the three coal powder streams used for staged combustion in the cone section have a faster average volatile matter release rate (Figure 7), but a lower volatile matter combustion rate (Figure 8), due to insufficient oxygen in the cone section.

From Figure 8 it can be observed that the average temperature near the coal pipes used for staged combustion in the cone part is higher than the average temperature near the main coal pipe in the cylinder part. This is because in the cone part, only a small part of raw meal undergoes chemical decomposition and absorbs heat, which is far less than that in the cylinder part.

The simulation results show that the burnout rate of the pulverized coal streams sprayed from the main coal pipe near the tertiary air inlet is 100%, while the burnout rate of the pulverized coal streams far from the tertiary air inlet is 97%. Among the pulverized coal streams sprayed from the three coal pipes used for staged combustion in the cone section, two have a 100% burnout rate and the other has a 98% burnout rate.

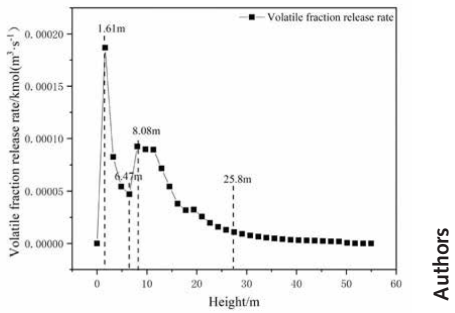

Authors

7 The release rate of volatile matter

5.4 Raw meal decomposition

For the decomposition of raw meal, since more than 80% of the raw meal is $CaCO_3$, only the decomposition reaction of $CaCO_3$ in the raw meal is considered in this paper. Figure 9 and Figure 10 show the concentration contour of $CaCO_3$ and CaO in the central longitudinal section at X=0 and Z=0, respectively. As can be seen from Figure 9(a) and Figure 10(a), the four streams of raw meal fall into the precalciner and move upwards soon carried by the gas streams, and the concentration of calcium carbonate gradually decreases while the concentration of calcium oxide gradually increases due to chemical decomposition (Figure 9(b) and Figure 10(b)). From Figure 9(b) we can see that the raw meal below falls into the precalciner and rapidly decomposes, as the area is a combustion area of coal combustion with high heat. In contrast, the decomposition path of raw meal falling from above is longer because the area is the post combustion zone of coal powder, with relatively less heat.

There is still a small part of raw meal not decomposed completely, after entering the gooseneck tube. Finally a small part of unreacted $CaCO_3$ escapes from the outlet.

In order to reflect the decomposition reaction of calcium carbonate more intuitively, the average mole fractions of $CaCO_3$ and CaO along Y direction were made, as shown in Figure 11. From Figure 11 we can see that with the raw meal falling into the

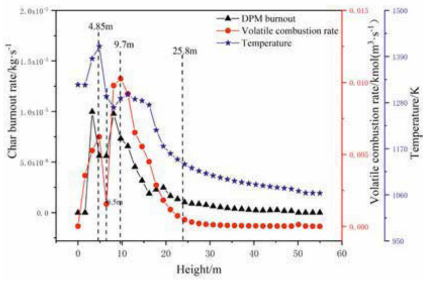

Authors

8 Average volatile kinetic reaction rate, char burnout rate and temperature along Y direction

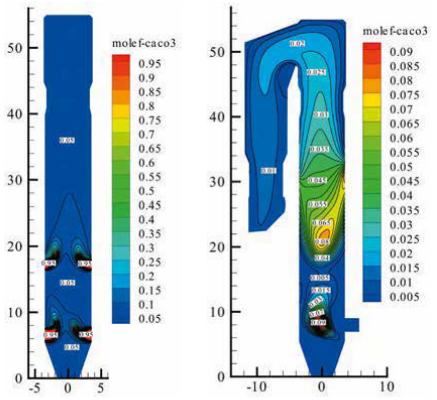

Authors

9 Mole fraction of CaCO3 on central longitudinal section of precalciner (a) z=0 (b) x=0

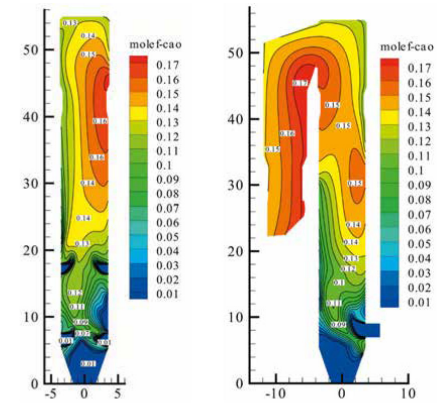

Authors

10 Mole fraction of CaO on central longitudinal section of precalciner (a) z=0 (b) x=0

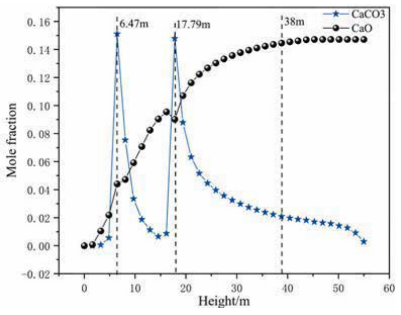

Authors

11 Average mole fractions of $CaCO_3$ and CaO along Y direction

precalciner from two different heights, two peaks of calcium carbonate concentration appeared along the height direction of the precalciner. The raw meal at the lower position reacts more quickly because there is more heat. The reaction rate of the raw meal at the higher position is relatively fast at the beginning, and then gradually slows down until the raw meal escapes from the precalciner. The calculated decomposition rate of $CaCO_3$ is 96%.

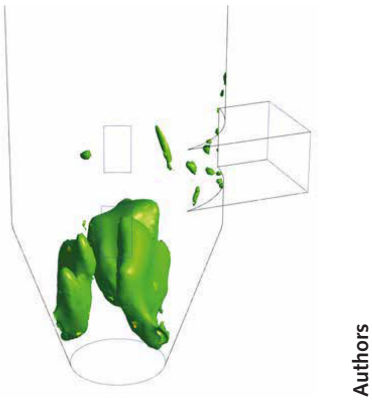

Authors

12 Iso-surface with CO molar concentration of 0.0003

5.5 NO distribution

In order to investigate the reducibility of the pulverized coal used for staged combustion, only the NOx carried in the flue gas is considered.

Figure 12 shows the iso-surface with CO molar concentration of 0.0003, which can indicate the shape of the flame. As shown in Figure 12, due to insufficient oxygen, more CO is generated during the combustion of the coal powder injected from the cone for staged combustion, which can effectively reduce the NO entering from the bottom of the precalciner.

Figure 13 shows the iso-surface with NO molar concentration of 0.0005, Figure 14 shows the Contour map of species concentration on central longitudinal section of CO and NO, and Figure 15 shows the contour map of species concentration at a height of y = 5 m. Combining Figure 13 to Figure 15 to analyze the process of nitrogen oxides reduction in the flue gas entering from the bottom of the precalciner. It can be seen that nitrogen oxides enter the bottom of the precalciner with flue gas, initially with a high concentration. However, when passing through the high CO

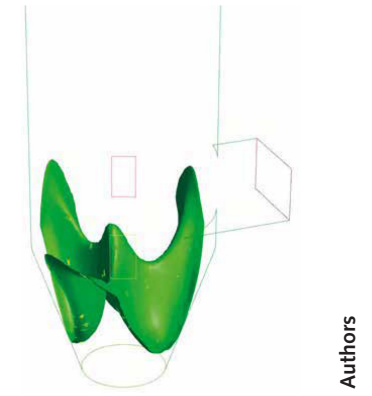

Authors

13 Iso-surface with NO molar concentration of 0.0005

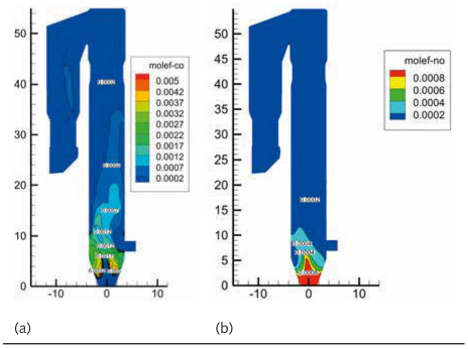

Authors

14 Contour maps of species concentration on central longitudinal section (a) CO (b) NO

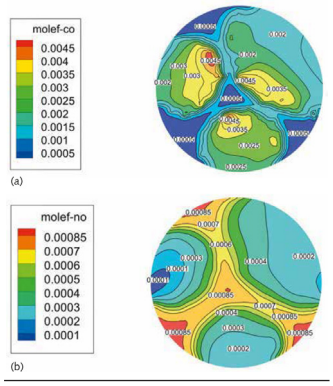

Authors

15 Contour maps of species concentration at a height of Y=5 m a) CO (b) NO

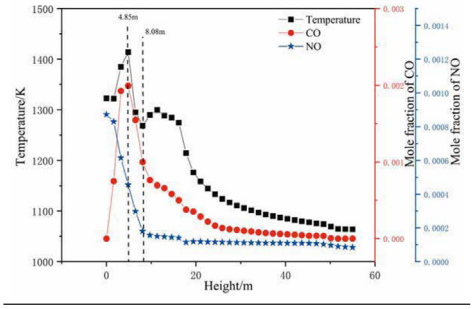

Authors

16 Average species concentrations of CO and NO and average temperature along Y direction

concentration zone generated by the coal staged combustion located in the cone section, nitrogen oxides are rapidly reduced and the concentration drops sharply. As shown in Figure 15, in areas with high CO concentration, the concentration of NO is relatively low.

Figure 16 displays the average species concentrations of CO and NO and average temperature along Y direction. As shown in Figure 17, when the height of the precalciner is less than 8.08 m, a large amount of CO is generated due to incomplete combustion of the coal powder in the cone. When NOx flows through this area, it is quickly reduced, resulting in a rapid decrease in its concentration to a lower value; When the height of the precalciner is greater than 8.08 m, the addition of tertiary air makes the coal powder burn more fully, resulting in a relatively small amount of CO generation. On the other hand, the concentration of remaining NOx has already decreased relatively low, so the degree of NOx reduction is very low there.

6 Conclusion

In this paper, the numerical simulation was carried out for a precalciner of the China Resources Cement Plant. The simulation results are consistent with the measured data, which shows the reliability of the simulation results. The simulation results are shown below.

(1) The flue gas enters the precalciner vertically from the bottom, while the tertiary air tangential enters the precalciner from the side, producing a "spouting effect" and a "swirling effect", respectively. Under the combined effect of the two effects, the two types of gas streams are well intertwined and spiral upward in the column, resulting in a long gas residence time.

(2) The pulverized coal in the precalciner is fully burned. The burnout rate of the pulverized coal streams from the main coal pipe near the tertiary air inlet is 100%, while that far from the tertiary air inlet is 97%. Among the pulverized coal streams sprayed from the three coal pipes used for staged combustion in the cone section, two have a 100% burnout rate and the other has a 98% burn out rate. The decomposition of raw meal is good, with a decomposition rate of up to 96%.

(3) When the pulverized coal streams used for staged combustion in the cone part enter the precalciner, incomplete combustion occurs due to low oxygen content, generating a large amount of CO, which rapidly reduces the nitrogen oxide entering from the bottom of the precalciner, indicating significant reduction in nitrogen oxide emissions.

Acknowledgements

This research was funded by National Key R&D Program of China (Grant No. 2024YFF0508300).

REFERENCES

[1] Chkheidze V. Local Raw Material, Fuel and Clinker Production Processing with 5 Stage PreCalciner Kiln and Grate Cooler in Georgia[J]. 2021.
[2] Bai T, Sun B, Guo Y, et al. Effects of tertiary air staged combustion on NOx emission characteristic in a pulverized-coal boiler with swirl burner[J]. Lecture Notes in Electrical Engineering, 2012, 155: 255–263.
[3] Ma H. K, Hsieh D. M, The reduction of thermal nitrogen oxides (NOx) emission using staged combustion in Furnace[J]. Journal of Thermal Science, 1993, 2(1): 61–69.
[4] Kolyfetis, E. Vayenas, C. G. mathematical modelling of separate line precalciners SLC. ZKG International, 1988. 41(11). 559-563
[5] Weilin Z, Bo W. Mathematical modelling of the turbulent flow field in a calciner[J]. Journal of Shandong Institute of Building Materials, 2001(01): 26-29
[6] X L, Xiaojia W. The study on thermal numerical simulation of cement kiln NC-SST-I precalciner[J]. Electric Power Technology and Environmental Protection, 2019.
[7] Xin C, Yongliang M. Numerical simulation of flow and temperature field in a cement precalciner[J]. Chinese Journal of Environmental Engineering, 2014.
[8] YU Y, Chenyang R, Yun L, et al. Numerical simulation of coupled CaCO3 decomposition by lignite combustion in a ducted calciner[J]. Bulletin of The Chinese Ceramic Society, 2019, 38(01): 27-32

[9] Li D, He X, Peng X, et al. Experimental study and CFD modeling of NOx reduction and reductive gas formation in deep reburning of cement precalciner[J]. Fuel Processing Technology, 2022, 229: 107183
[10] Bugge, M., et al. Numerical Simulations of Staged Biomass Grate Fired Combustion with an Emphasis on NOx Emissions. Energy Procedia, 2015. 75: p. 156-161.
[11] Zeng X, Chen X, Yi Z, et al. Formation characteristics of self-generated nitrogen oxides in a cement precalciner[J]. ZKG Cement Lime Gypsum, 2022 (3):75.
[12] Yang Y, Zhang Y, Li S, et al. Numerical simulation of low nitrogen oxides emissions through cement precalciner structure and parameter optimization[J]. Chemosphere, 2020, 258:127420.
[13] Shengqiang K E. Effect of pulverized coal injection proportion on NOx in NST precalciner[J]. Cement, 2018.